

ELECTRON DENSITIES IN PLANETARY NEBULAE

LETIZIA STANGHELLINI AND JAMES B. KALER

Department of Astronomy, University of Illinois

Received 1988 December 19; accepted 1989 January 27

ABSTRACT

Electron densities for 146 planetary nebulae have been obtained by analyzing a large sample of forbidden lines ([O II], [Cl III], [S II], and [Ar IV]) by interpolation of theoretical curves obtained from solutions of the 5-level atoms, with up-to-date collision strengths and transition probabilities. Electron temperatures were derived from the [N II] and/or the [O III] lines, or were estimated from the He II $\lambda 4686$ line strengths. Inhomogeneities in the nebulae make comparisons among different data sets difficult. Although the averaged data show considerable scatter, we still see that [O II] densities are generally lower than those from [Cl III], by an average factor of 0.65. The agreement between [O II] and [S II] for all data is good, with N_e [O II] lower by only 0.95. If we restrict ourselves to observations from data sets in which [O II] and [S II] were observed in common (which minimizes the effect of inhomogeneities), the [O II] values drop to 0.84 that of the [S II], implying that the outermost parts of the nebulae might have elevated densities. The scatter is large, however, and the difference is only marginally significant. The [Cl III] and [Ar IV] densities show the best correlation, especially in the case that these densities have been obtained from common data sets. The [Ar IV] densities are somewhat lower than those from [Cl III], implying that on the average Ar^{+3} may be produced in a central hole. These differences, however, could all be considered to be caused by small errors in the atomic parameters. Under the assumption that we have homogeneous nebulae, the current atomic data still give results within 30% of one another, a very satisfactory situation. The [Ar IV] electron densities now appear to give reasonable results and are especially useful at high densities where the [O II] and the [S II] curves become flat. Although the data are sparse, there is no evidence that recombination plays a role in the production of the [O II] lines.

Subject headings: nebulae: planetary

I. INTRODUCTION

The importance of acquiring physical data on planetary nebulae (PNe) is increasing, considering the fundamental role that these objects play in stellar and galactic evolution. In particular, the calculation of chemical abundances, the construction of nebular models, and the study of the influence of the evolution of the central star on that of the nebula, including the effect of the stellar wind, requires a knowledge of the electron densities of the nebulae. The intensities of various forbidden, collisionally excited lines in planetary nebulae (ground-state doublets of [O II], [S II], [Cl III], and [Ar IV]) are commonly used to obtain these densities. The use of different ions, together with the availability of a large number of spectral line intensities in the literature, then allows a detailed comparative and analytic study of these densities.

Comparisons among electron densities in planetary nebulae as obtained from different ions have been made principally by Saraph and Seaton (1970) and by Aller and Epps (1976). The calculations in the earlier paper included a sample of 11 planetary nebulae for which densities were calculated from the [O II], [S II], [Cl III], [Ar IV], and [K V] forbidden lines ratios. The authors found that the [Ar IV] and [K V] densities are generally in disagreement with the others, which they ascribed to the variations of densities on a large scale. They also found the [S II] densities to be high relative to those derived from [O II]. Aller and Epps then analyzed a sample of gaseous nebulae for which the [O II] densities had already been calculated, and also found the [S II] values to be slightly higher than those from [Cl II] and [O II]. This result suggested that the S^+ spectral lines might be produced in denser regions than are either the O^+ or Cl^{+2} lines.

In the last two decades, several spectrographic surveys have been made of PNe, which together with various data published earlier, provide a sample of 146 objects for analysis. And since the publication of the compilation of atomic parameters by Mendoza (1983), improved transition probabilities have become available for [O II] (Zeippen 1987) and new collision strengths have been calculated, for [Ar IV] (Zeippen, Butler, and LeBourlot 1987) and [Cl III] (Butler and Zeippen 1989). Consequently, a new detailed examination is in order.

The improved atomic data are of particular importance in a new examination of electron densities. The large sample of observed spectral lines employed in this study provides a good basis with which to explore the differences among electron densities as calculated from different ions and gives us a possibility of checking whether some discrepancies that exist among electron densities are due to the structures of the nebulae, or to the reliability of the atomic calculations.

II. METHOD

The spectral lines suitable for plasma diagnostics that enable the calculation of electron densities are those produced by the $2p^3 \text{O}^+$ ion and by the $3p^3 \text{S}^+$, Cl^{+2} , and Ar^{+3} ions. The specific doublets of interest are [O II] $\lambda 3727\text{--}3729$, [Cl III] $\lambda 5517\text{--}5537$, [S II] $\lambda 6717\text{--}6730$, and [Ar IV] $\lambda 4711\text{--}4740 \text{ \AA}$. The electron densities were calculated from the observed ratios of the doublet intensities and the theoretical curves of ratio versus density that were obtained by solving the balance equations for the 5-level p^3 ion. Figures 1 to 4 show these theoretical intensity ratios for each doublet for $T_e = 10^4 \text{ K}$ plotted against the logarithm of the electron density. The curves are shifted only slightly for other temperatures.

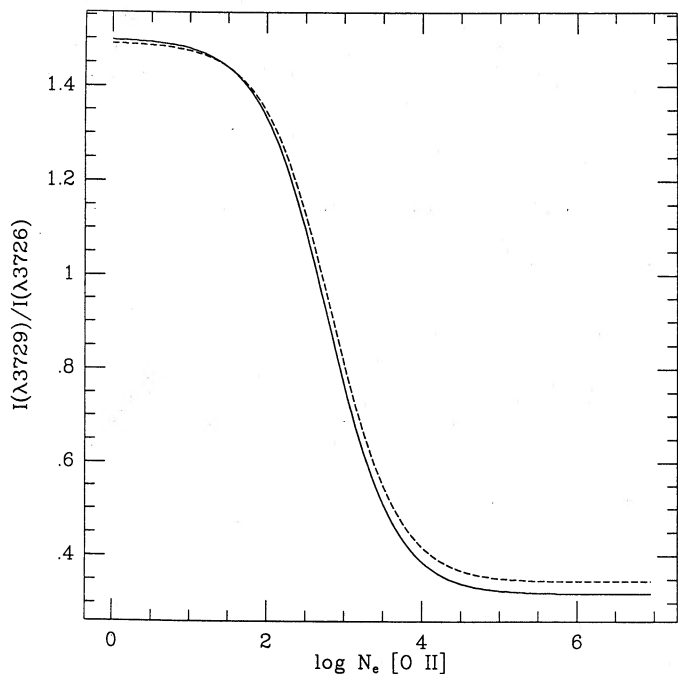


FIG. 1

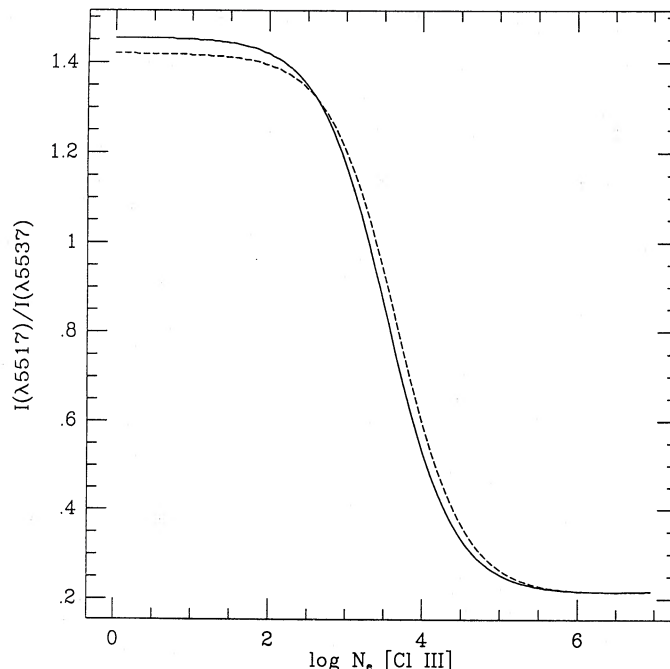


FIG. 2

FIG. 1.—Theoretical intensity ratio for [O II], $I(\lambda 3729)/I(\lambda 3726)$ vs. $\log N_e$, calculated for $T = 10^4$ K. Collisional strengths from Pradhan (1976). Transition probabilities: dashed line from Zeppen (1982); solid line from Zeppen (1987).

FIG. 2.—Theoretical intensity ratio for [Cl III], $I(\lambda 5517)/I(\lambda 5537)$ vs. $\log N_e$, calculated for $T_e = 10^4$ K. Collisional strengths: dashed line from Krueger and Czyzak (1970); solid line from Butler and Zeppen (1988). Transition probabilities from Mendoza and Zeppen (1982).

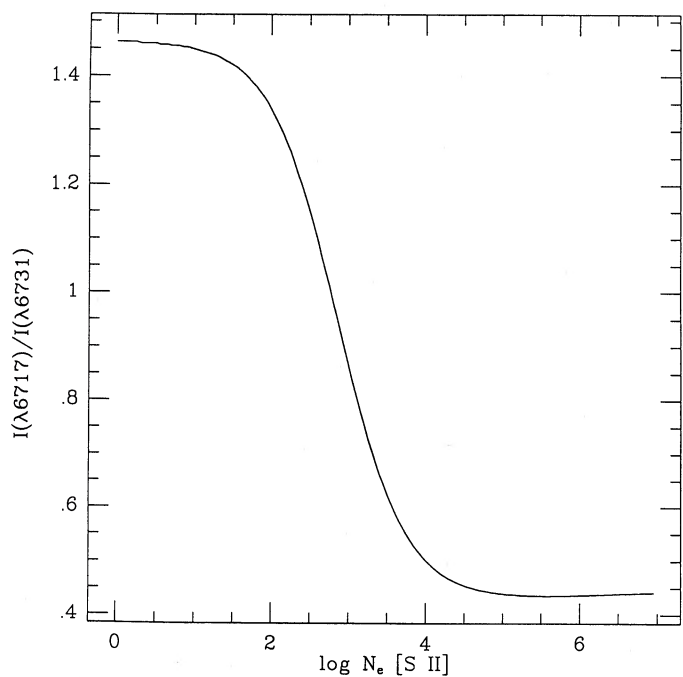


FIG. 3

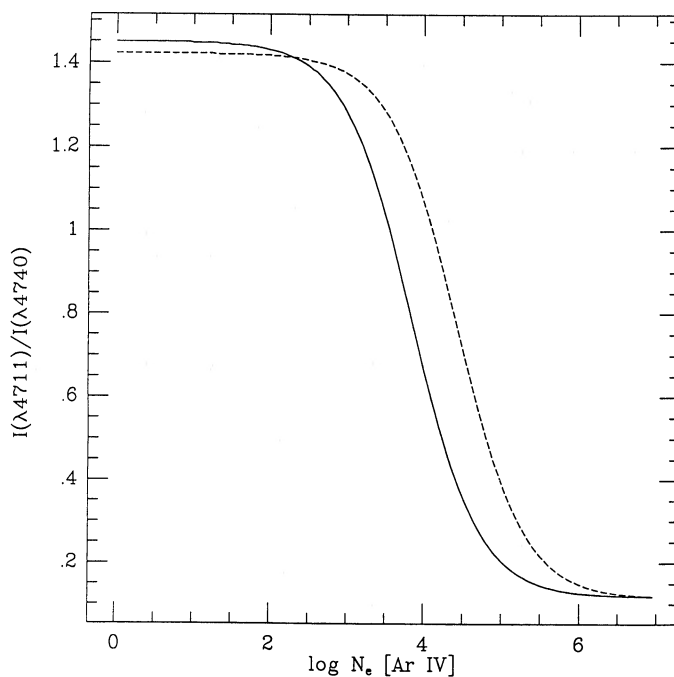


FIG. 4

FIG. 3.—Theoretical intensity ratio for [S II], $I(\lambda 6717)/I(\lambda 6731)$ vs. $\log N_e$, calculated for $T_e = 10^4$ K. Transition probabilities from Mendoza and Zeppen (1982). Collisional strengths from Mendoza (1983).

FIG. 4.—Theoretical intensity ratio for [Ar IV], $I(\lambda 4711)/I(\lambda 4740)$ vs. $\log N_e$, calculated for $T_e = 10^4$ K. Transition probabilities from Mendoza and Zeppen (1982). Collisional strengths from Zeppen, Butler, and LeBourlot (1987).

The broken curves correspond to the use of the "old" atomic data (Mendoza 1983), while solid lines refer to the improved collision strengths and transition probabilities cited above (see also the figure captions for references). The latter sets of atomic data, and the corresponding ratio-density curves, have been used to calculate the electron densities presented in this paper. We can see from Figure 4 that the use of the new collisional strengths for [Ar IV] significantly changes the density domain for which the Ar^{+3} ion can be used. The curve is pulled to the left so that in the middle of the range the [Ar IV] densities will now be about 0.5 dex lower than before. The oxygen and the chlorine curves, in Figures 1 and 2, show their domains to be substantially unchanged. For [S II], no new atomic data are available.

The limiting ratios for high density, which depend on the ratio of transition probabilities, can be extracted from Mendoza and Zeppen (1982) for the [Cl III], [S II], and [Ar IV] spectra, while the limiting ratio for high density for [O II] is from Zeppen (1987). The lower limit to the electron densities, which depends on the ratio of collision strengths, corresponds to the flat portion of the model curves, near the left part of the plots. In principle (if all the lines are present) we can perform plasma diagnostics for the wide range of densities from approximately 10^2 to 10^7 cm^{-3} .

However, one must be very aware of the problem posed by the density limits. If an observed ratio is near a limit, a small observational error can give a seriously erroneous answer. Electron densities near the limits can be then very unreliable. This problem especially affects those derived from [Ar IV], since that curve falls in the upper range of planetary densities and the data are often the least reliable (see below), that is, it is easy to obtain a false high value. As an example, the low-density limit is $I(\lambda 4711)/I(\lambda 4740) = 1.45$. If the observed ratio is 20% too low, not an unrealistic error, we would obtain $N_e = 2 \times 10^3$ for a nebula whose real density was far below that. In order to account for this effect, and to establish realistic ranges over which the densities should be reasonably reliable, we assume that all data will be in error by $\pm 20\%$. The curves in Figures 1 through 4 should then properly be used from 20% below the upper limit to 20% above the lower. For each ion these ranges are: $\log N_e$ [S II] from 2.45 to 3.85; $\log N_e$ [O II] from 2.4 to 4.05; $\log N_e$ [Cl III] from 3.0 to 4.95; and $\log N_e$ [Ar IV] from 3.3 to 5.55. Figure 5 shows all the curves presented together with these "acceptable" ranges drawn with solid lines.

The [O II] and [S II] densities are based on electron temperatures found from [N II]; the other two are derived from T_e [O III]. Most are taken from Kaler (1986). When these are not available, we calculate them from the referenced data, using the formulae also from Kaler (1986). When the actual electron temperatures are not known, we adopt estimates from the strength of the He II $\lambda 4686$ line and Kaler's (1986) calibration. These new values are shown in Table 1. The last column of the table shows the method of calculation. The actual grid used for the calculation contains an option of choosing among three values of the electron temperature: $T_e = 5000$, $T_e = 10,000$, and $T_e = 20,000$ K. The differences among the theoretical intensity ratios for the same value of the density, and for $\Delta T = 5 \times 10^3$ K, is only of the order of few thousandths, so there is no need to interpolate among the electron temperatures.

In the calculation of N_e from the [Ar IV] lines, we had to take into account the fact that most references give the intensity of $\lambda 4711$ blended with that of He I $\lambda 4713$. We separate the

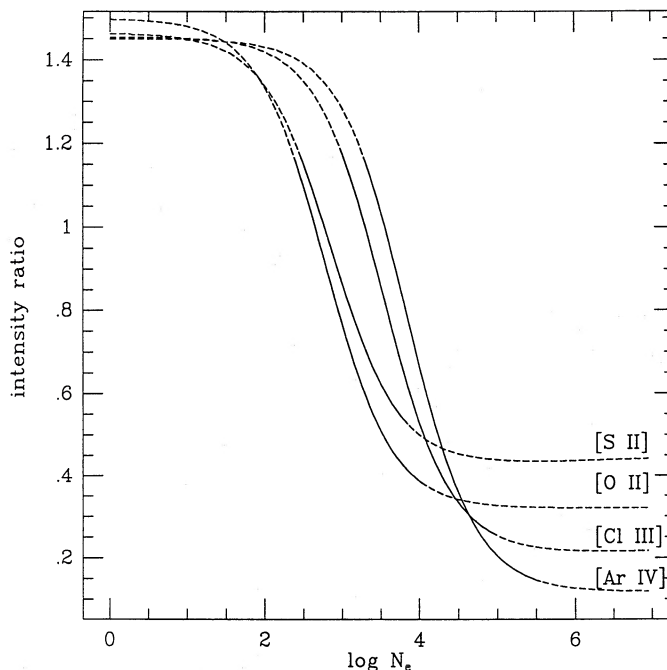


FIG. 5.—All theoretical curves, with solid lines corresponding to reliable portions, and broken lines corresponding to less reliable portions. The broken lines are the parts of the curves that lie within 20% of the flat portions.

TABLE 1
CALCULATED ELECTRON TEMPERATURES

Name (1)	T_e [N II] (2)	T_e [O III] (3)	Method and Notes (4)
NGC 1535	11100	...	From T_e [O III], Kaler 1986
NGC 2022	10400	...	From T_e [O III], Kaler 1986
NGC 2346	12900	...	From spectral lines
NGC 3587	7600	...	From spectral lines
NGC 6445	10100	12800	From spectral lines
NGC 6741	14700	17500	From spectral lines
NGC 6891	15100	14200	From spectral lines
NGC 7008	7800	12200	From spectral lines
IC 351	10100	...	From T_e [O III], Kaler 1986
IC 1747	6600	...	From spectral lines
IC 3568	11100	...	From T_e [O III], Kaler 1986
IC 4997	20000	20000	Assumed
Cn 2 1	10400	10000	From 4686 Å
Hb 6	10000	10700	From spectral lines
Hb 12	22000	25700	From spectral lines
K 3 61	10200	10300	From 4686 Å
M 1 4	12300	...	From T_e [O III], Kaler 1986
M 1 6	11400	23900	From spectral lines
M 1 8	16100	18500	From spectral lines
M 1 9	13700	16000	From spectral lines
M 1 11	22800	21900	From spectral lines
M 1 16	14200	11900	From spectral lines
M 1 33	13100	12600	From spectral lines
M 1 65	23500	22600	From spectral lines
M 1 80	9600	12700	From spectral lines
M 3 20	10400	9700	From 4686 Å
Me 1 1	10400	10000	From 4686 Å
Na 1	10500	10900	From spectral lines
Sn 1	10500	...	From T_e [O III], Kaler 1986
Vy 1 1	15900	15600	From 4686 Å
Vy 2 3	10300	10300	From 4686 Å
P 33 (LMC)	10100	11500	From 4686 Å

helium and argon lines by assuming that the helium contribution to the blend is one-tenth of the intensity of He I $\lambda 4471 \text{ \AA}$ (Brocklehurst 1971), after correction for reddening. The subtraction significantly increases the error of the ratio, which may already be fairly high because of the weakness of the lines. The [Cl III] lines are usually even weaker, with concordantly higher error. The [S II] and [O II] lines are strong, however, and should be reasonably free of random error. The actual errors in density are not possible to estimate since the observations are from such a variety of sources, and since observational errors are rarely quoted. As a result it is reasonable simply to adopt $\pm 20\%$ for all data as proposed above.

III. RESULTS

We present a list of all calculated electron densities in Table 2. Column (1) gives the name of the object (NGC, IC, then alphabetic) and column (2) the reference to the observed spectral lines. Some of the observed intensities come from more than one region in the nebula; in that case, a region key is listed with the reference. A key to references and regions is given at the end of the table. Columns (3), (4), (5), and (6) then give the logarithmic electron densities calculated from the [S II], [O II], [Cl III], and [Ar IV] spectral lines, respectively. The last entry for each nebula in the case of an object with multiple entries, and called "AV" in the reference column, refers to the density calculated from the average intensity ratio (it is not the average of the densities). *We give the density results regardless of whether or not the result is near the density limit. The density should be viewed with suspicion unless it is actually inside the allowed domain given in the last section and in Figure 5.*

Our goal is the comparison of the density derived from one ion with that derived from another. The large sample of objects analyzed, together with this statistical study, give some guidelines in the choice of the electron densities that will give the best representation and the best means. By looking at several individual objects we can see that making a general statement about the behavior of electron densities can be a difficult task because of their varied structures. We examine a few nebulae in particular below, where we reject, or comment on, various data sets.

NGC 650.—The [O II] data by Minkowski and Osterbrock (1960) refer to a very low density envelope, and a slightly denser bar. These data are not included in the comparison analysis. The [Ar IV] and [Cl III] electron densities are larger, and, in the case of [Ar IV], are not homogeneous through the nebular gas. The [Ar IV] density is not reliable, since the corresponding intensity ratio is close to the lower reliability limit of the curve. The [S II] value then seems to be the most appropriate for this nebula.

NGC 2371.—The oxygen entry refers to the envelope of the nebula, which is considerably fainter than the inner parts; the corresponding electron density datum is not included in the comparative analysis. The lowest electron density, calculated from [Ar IV], is close to limit of reliability of the curve.

NGC 2440.—Refer to the original spectral line reference (BR), which includes a picture of this object, and note that region F2 is the closest observation to the center of the nebula, while the other, lower, sulfur electron densities come from the outer part of the object.

NGC 2452.—All the [O II] electron densities are consistently lower than the one from other ions. It seems likely that the

oxygen lines are emitted from an outer, lower density zone in the nebula.

NGC 3587.—Considerable point-to-point density variations are seen. The chlorine and sulfur lines were observed within the inner zone of ionization; the strong difference between these latter electron densities might be due to an ionization gradient along the line of sight, where the [Cl III] is coming from an inner zone of higher density.

NGC 6445.—Data from (AE2) refer to the brightest part of the object. Differences in N_e between the zones can probably be ascribed to a density gradient.

NGC 6720.—Most data give a very low N_e [O II], [Cl III], and [S II], while N_e [Ar IV] is discordant; the latter density is, for the reference C, region 4, at the limit of reliability. These results exemplify the problem with density limits discussed in the previous section. The very low density is clearly the more acceptable.

NGC 6751.—The intensities of the chlorine spectral lines are very low, with a likely error of a factor of 2. A better value for the electron density of this object is the one derived from the sulfur lines, which are two orders of magnitude more intense than the chlorine lines.

NGC 6778.—The sulfur and argon lines are both stronger than chlorine lines.

NGC 7008.—The sulfur lines correspond to a peculiar zone of the nebula.

NGC 7027.—The [Cl III] electron density is very unreliable, close to the upper density limit for this ion.

NGC 7293.—This is a very low density object. The 1960 data give the oxygen intensities in the outer ring, which is fainter. The sulfur electron density (HAW2; B2) is at the lower reliability limit of the curve.

IC 418.—Both N_e [O II] (SO) and N_e [S II] (AW70) are at the limits of reliability.

IC 5117.—The data set from (AC79) gives a more uniform electron density than that from (AE2). The sulfur electron density is close to limit of reliability for the former reference.

Finally, for IC 4634, IC 4776, IC 4997 (AE2), M1-4 (AE2), and M1-74, the sulfur electron density is close to the limit.

Tables 3 and 4 now present averages of the data in order that we may compare densities derived from different ions. The analysis is broken into two parts. In Table 3 we examine the data in which the line intensities were derived from all sources. From Table 2 we see that densities for different ions derived from different data sets can be quite discordant, up to a maximum of an order of magnitude, while most of the densities that are derived for a given nebula from the same data set are generally in reasonably good agreement. Because of stratification, and because different observers choose different nebular positions, the densities may not correspond well to one another, increasing the errors in the comparisons. In Table 4 we therefore list higher quality ratios, where the densities are derived for a single location from single-source data. Comparisons among densities are given in the tables by the formula

$$C(X, Y) = \left\{ \sum_{i=1}^N [N_e(X)/N_e(Y)]_i \right\} / N, \quad (1)$$

where $C(X, Y)$ is the ratio of the densities for ions X and Y . In Table 3, $N_e(X)$ and $N_e(Y)$ are the averages in Table 2 (AV) for individual nebulae, and N is the number of objects. In Table 4 they are individual values observed in common from single sources and N is the total number of observations. That is, to be included in the mean ratios of Table 4, both densities must

TABLE 2
 ELECTRON DENSITIES

Nebula (1)	Ref (2)	[S II] (3)	[O II] (4)	[Cl III] (5)	[Ar IV] (6)	Nebula (1)	Ref (2)	[S II] (3)	[O II] (4)	[Cl III] (5)	[Ar IV] (6)	
NGC 40	ACBL	...	2.95	NGC2392 (cont.)	AC79	3.55	...	2.59	...	
	AUV	...	2.84		AE2 1	3.57	...	2.89	...	
	OS T	...	3.01		AE2 2	2.97	...	3.30	...	
	OS R	...	3.06		AW70 A	3.29	...	
	AC79	3.04	...	3.32	...		AW70 B	3.65	...	
	AE2	3.29	...	3.32	...		BR F1	3.05	...	2.91	...	
AV	3.16	2.96	3.32	...	BR S1		2.78	...	3.47	...		
NGC 650	MO B1	...	1.97		BR F2	2.92	
	MO B2	...	2.25		BR S2	2.78	
	MO B3	...	2.40		MA 1	3.45	
	MO B4	...	2.27		MA 2	3.17	
	MO B5	...	2.25		MA 60	2.96	
	MO E1	...	1.90		MA 3	3.66	
	MO E2	...	1.97		AV	3.02	3.18	3.21	3.35	
	AV, BAR	...	2.24		NGC2440	OS	...	3.22
	AV, ENV	...	1.94			AE2	3.41	...	3.74	...
	C 2	3.60	3.78			AKCS	3.54	...	3.66	...
	AC83	2.54			AW70	3.50	...
	AC79	2.54			BR F	2.96
	AE2 1	2.51			BR F1	2.76
	AE2 2	2.73			BR F2	3.04
C 1	4.07	BR F3			2.51	
C 3	2.45	BR S			2.16	
AV	2.51	2.16	3.60	3.63	BR S1			1.91	
NGC1501	AE2	3.17			CAK1 C	4.12
								CSAS A	3.81
NGC1535	AC79	...	3.40	...	3.03			CSAS B	3.75
	ACPG	...	3.20			LA	3.65
	AW	...	3.39		MA MW	3.47	
	MA R	3.02		AV	2.81	3.22	3.63	3.77	
	AV	...	3.33	...	3.03		NGC2452	AC79 A	3.35	2.88	3.21	2.94
NGC2022	AC70	...	2.87	...	3.53			AC79 B	3.54	2.97	3.57	3.86
	AC79	3.24	2.88	3.05	3.17	AKI C		...	2.97	...	2.99	
	AC83	3.20	2.78	3.11	...	AKI E		...	2.88	...	3.18	
	AW	...	3.22	AC79 C		3.24	...	2.91	3.06	
	AW70	2.91	...	AE2		3.46	
	AE2	2.69	AV		3.39	2.92	3.26	3.28	
	MA	2.61	NGC2474		DOK	2.15
	AV	3.03	2.93	3.22	3.21		NGC2867	AKRM	3.24	...	3.85	3.29
NGC2346	AC79	...	2.47	NGC2899		RM	2.76
	AKI PG	...	2.48		NGC3132	AKI	...	2.63
	SAB2	2.79	NGC3242		CAKF	...	3.53
	AV	2.79	2.47		OS	...	3.08	
NGC2371	ACPG E1	...	1.82	...	3.42		AC79	3.42	...	3.51	3.55	
	AE2	3.14	...	3.37	...		AE2	3.94	...	3.61	...	
	AC83 1	2.92	...	3.23	...		AW70	3.36	...	
	AC83 2	3.09	...	3.37	...		BR F	3.18	...	2.92	...	
	AC79	3.32	3.42		BR S	3.56	...	
	ACPG F	2.82		AV	3.45	3.27	3.41	3.55	
AV	3.11	1.82	3.34	3.28	NGC2392	AH	...	3.65		
NGC2392	ZI2	2.73	2.86						

TABLE 2—Continued

Nebula (1)	Ref (2)	[S II] (3)	[O II] (4)	[Cl III] (5)	[Ar IV] (6)	Nebula (1)	Ref (2)	[S II] (3)	[O II] (4)	[Cl III] (5)	[Ar IV] (6)
NGC3587	OS A	...	1.92	NGC6445	(cont.)				
	OS B	...	1.77		AE2	3.16	...	3.47	...
	OS C	...	1.69		ACCK	3.30
	OS D	...	1.98		AV	3.16	2.73	3.47	3.30
	OS E	...	2.11	NGC6537	ACPG	...	3.26	...	4.19
	OS F	...	1.81	NGC6543	CAK2	...	3.40
	OS G	...	2.03		AH	...	3.48
	OS H	...	1.85		AUV	...	3.53
	BR	2.22	...	3.66	...		BCA CS	...	4.20
	AV	2.22	1.91	3.66	...		BCA F3	...	3.82
NGC3918	TPP	3.73	3.70		BCA F4	...	4.00
	AF	3.87		BCA F5	...	3.95	...	3.51
	AV	3.73	3.79		BCA F6	...	3.73
NGC4361	HAC PG	...	3.83		BCA PE	...	3.93
NGC5315	TPP	4.29		BCA S1	...	3.85
NGC6058	ACPG	...	3.26		BCA S2	...	3.92
NGC6210	ACB	...	3.67	...	3.72		BCA S3	...	3.51	...	2.85
	AC83	...	3.67	3.54	...		BCA S4	...	3.57
	AH	...	3.48		BCA S5	...	3.97	...	3.70
	AUV	...	3.67		CAK2 WK	...	2.63
	BAR	3.51	3.64		DG75 C1	...	3.73
	LU	...	3.44		DG75 S1	...	3.01
	AE2	3.42	...	3.48	...		DRS	...	3.57
	FR1	3.50	3.52		LU	...	3.51
	C	3.88		AC79	3.55	...	3.67	3.30
	AV	3.48	3.58	3.51	3.71		AE2	3.98	...	3.80	...
NGC6302	OA A	...	3.55	...	4.13		AW70 CB	3.86	...
	OA C	...	3.39	...	3.54		AW70 KA	3.58	...
	OA D	...	3.18	...	3.99		AW70 KB	3.80	...
	OA E	...	3.45	...	4.16		DG75 C2	3.75	...
	OA F	...	3.05	...	3.98		DG75 C3	3.84	...
	AE2	4.17	...	4.57	...		DG75 NE	3.76	...
	AW70	4.64	4.12		DG75 S2	3.25	...
	AV	4.17	3.31	4.61	3.99		DG75 SW	3.82	...
NGC6309	AW 1	...	3.06		BCA	2.55
	AW 2	...	3.33		WD	3.56
	AW 3	...	4.15		BCA S6	3.88
	CA70 C	...	3.38	...	3.27		LU2	3.68
	CA70 C2	...	3.32	...	3.06		O	4.05
	CA70 O	...	3.00	...	3.40		AV	3.29	3.54	3.71	3.61
	AC83	3.59	3.37	NGC6565	AKI	...	2.47
	AE2	3.33	...	3.40	...	NGC6567	ACPG	...	3.21
	AW70	3.68	...		AK83	4.42	...	3.77	...
	AV	3.38	3.30	3.54	3.25		BAR	4.10
NGC6369	AK83	3.81	...	4.01	...		AV	4.22	3.21	3.77	...
NGC6445	ACCK AV	...	2.78	NGC6572	AH	...	3.70
	ACCK RM	...	2.93		AUV	...	3.73
	ACCK RL	...	2.52		AE2	4.31	...	4.06	...
	ACCK C	...	2.70		AW70	4.02	...
							AC79	4.02	4.12
							FR1	3.70	4.11
							NOS32	3.40
							WD	3.42

TABLE 2—Continued

Nebula (1)	Ref (2)	[S II] (3)	[O II] (4)	[Cl III] (5)	[Ar IV] (6)	Nebula (1)	Ref (2)	[S II] (3)	[O II] (4)	[Cl III] (5)	[Ar IV] (6)
NGC6572	(cont.)					NGC6778	AC79	2.93	...	3.22	3.21
	AK2	4.27		AE2 1	2.95	...	3.20	...
	A41	4.10		AC83	2.85	...	3.23	...
	LA	4.49		AE2 2	3.02
	OPC	3.75		AV	2.94	...	3.22	3.21
	AV	3.68	3.71	4.04	4.12						
NGC6629	AKI	...	3.14	NGC6781	AKI	2.71
NGC6644	AKI	...	3.67	...	4.36	NGC6790	AKI	...	3.68	...	4.16
	BAR	3.76		AC79	4.04	...	3.77	4.46
	AV	3.76	3.67	...	4.36		AE2	4.46	...
							FR1	3.98	4.31
NGC6720	DRS	...	2.77		A	3.98
	MO I1	...	2.47		AV	4.01	3.68	4.05	4.21
	MO I2	...	2.63	NGC6803	LAKC	...	3.72	3.86	3.88
	MO I3	...	2.56		OS	...	3.36
	MO R1	...	2.68		LAKC B	3.18
	MO R2	...	2.72		AV	3.18	3.51	3.86	3.88
	MO R3	...	2.65	NGC6807	AK83	4.37
	MO R4	...	2.68						
	MO R5	...	2.74	NGC6818	AC79	3.15	3.29	3.43	3.03
	MO R6	...	2.60		LU	...	3.36
	MO FN	...	2.33		AE2	3.26	...	3.32	...
	MO FS	...	2.20		AW70	3.64	...
	AV, RING	...	2.81		AV	3.20	3.32	3.47	3.03
	AV, ENV	...	2.27	NGC6826	CAK4	...	3.15
	AW70	2.73	...		AC83	3.43	3.15	3.50	...
	BAR4 1	2.79		LU	...	3.10
	BAR4 3A	2.87		AE2	3.53	...	2.65	...
	BAR4 4	2.88		AW70	3.58	...
	BAR4 6	2.79		BR F	3.97	...	3.01	...
	FR1	2.85	3.13		BR S	2.94	...	3.32	...
	HM 1	2.60		FR1	3.68
	HM 2	2.71		AV	3.44	3.14	3.26	...
	HM 3	2.72	NGC6833	AKI	...	3.63	...	3.04
	HM 4	2.76		AK83	3.99
	HM 5	2.54		AV	3.99	3.63	...	3.04
	HM 6	2.34	NGC6853	AKI E	...	2.48
	C 1	3.85		OS J	...	2.39
	C 2	3.81		OS K	...	2.37
	C 3	4.05		HM4 1	2.14
	C 4	2.78		HM4 2	2.37
	AV	2.72	2.60	2.73	3.61		HM4 3	2.35
NGC6741	AKRC	...	3.33	...	4.17		HM4 4	2.26
	AW	...	3.35		HM4 5	2.57
	LU	...	3.40		HM4 6	2.38
	AE2	3.97	...	3.96	...		SAB 2	2.64
	AW70	3.82	...		AKI C	3.80
	A	4.21		C	3.68
	AV	3.97	3.36	3.89	4.18		AKI M	3.43
NGC6751	AC79	3.51	...	2.34	...		AV	2.40	2.41	...	3.64
	AE2	3.49						
	AV	3.50	...	2.34	...						

TABLE 2—Continued

Nebula (1)	Ref (2)	[S II] (3)	[O II] (4)	[Cl III] (5)	[Ar IV] (6)	Nebula (1)	Ref (2)	[S II] (3)	[O II] (4)	[Cl III] (5)	[Ar IV] (6)
NGC6879	AK83	3.77	...	3.30	...	NGC7026	(cont.)				
NGC6884	AC79	3.84	3.74	3.68	3.99		AE2 2	3.35
	AKI	...	3.73		ORF	3.10
	LU	...	3.67		CA70 FM	3.75
	AE2	3.87	...	3.79	...		CA70 P	3.53
	AW70	3.71	...		AV	3.46	...	3.80	3.67
	A	3.76	NGC7027	AH	...	3.69
	R	3.67		AUV	...	3.69
	AV	3.86	3.72	3.73	3.81		KACE	4.80	...	5.11	...
NGC6886	AC79	4.01	3.57	4.04	3.68		WD	3.64
	LU	...	3.59		CSAS	4.97
	AE2	3.96	...	4.00	...		FR1	4.43
	AW70	3.99	...		O	3.85
	A	3.61		AV	3.94	3.69	5.11	4.30
	ACP	3.55	NGC7293	OS L	...	2.08
	AV	3.99	3.58	4.01	3.61		OS M	...	2.05
NGC6891	AKI	...	3.15		OS N	...	2.08
	LU	...	3.12		OS O	...	1.86
	C	3.47		OS P	...	2.02
	AV	...	3.13	...	3.47		HAW2 A2	2.60
NGC6894	AKI	...	2.65		HAW2 A4	2.06
NGC6905	AE2	3.02		HAW2 B2	2.45
	AC79	2.85		HAW2 B3	1.64
	AV	2.93		HAW2 B4	3.21
NGC7008	ACPG HB	...	3.94	...	3.02		WR X1	2.69
	AS B	...	3.50		WR X2	2.07
	AE2	2.89		WR X3	2.00
	C 2	3.35		WR X4	1.82
	C 4	3.35		WR X6	2.52
	AV	2.89	3.68	...	3.26		AV	2.34	2.02
NGC7009	AK1	...	3.19	NGC7662	AKB	...	3.38	...	3.54
	AUV	...	3.52		AC79	3.43	3.39	3.55	3.53
	CA79 1	3.67	3.51	3.75	...		LU	...	3.40
	CA79 2	3.73	3.64	3.58	3.64		MA C	...	3.40	3.83	3.74
	AE2 1	4.29	...	3.71	...		MA 2	...	3.21	...	3.61
	AE A	3.68	...	3.75	...		MA 3	...	3.15
	AE CB	3.68	...	3.69	3.64		MA 5	...	3.24	...	3.39
	AE2 2	3.77	...	3.58	...		MI71	...	3.25
	AW70 A	3.45	...		AC83	3.44	3.38	3.55	...
	AW70 B	3.58	...		AE2	3.42	...	3.29	...
	CA79 3	3.23		AW70 OE	3.38	...
	FR1	4.45	3.27		AW70 R	3.14	...
	WD	3.56		FR1	4.54	3.79
	AKI	3.93		NOS32	2.79
	CA7911	3.78		WD	3.52
	OPC	3.82		CSAS I	3.11
	LA	3.42		CSAS II	3.30
	AV	3.69	3.45	3.64	3.63		LA	2.96
NGC7026	AC79	3.98	...	3.62	3.71		MA 60	3.66
	AE2 1	3.73	...	4.00	...		MA 0	3.36
							TA M	3.57
							AV	3.39	3.31	3.46	3.49

TABLE 2—Continued

Nebula (1)	Ref (2)	[S II] (3)	[O II] (4)	[Cl III] (5)	[Ar IV] (6)	Nebula (1)	Ref (2)	[S II] (3)	[O II] (4)	[Cl III] (5)	[Ar IV] (6)
IC 351	AW	...	3.49	IC 4593	AUV	...	3.19
	AC83	3.29	3.56	3.34	...		BAR	2.80	3.26
	AC79	3.16	...	2.92	3.12		CEBA	3.16	3.14
	AW70	2.87	...		LU	...	3.19
	TPP	3.40		SO	...	3.22
	AV	3.22	3.52	3.07	3.28		AE2	3.20	...	3.85	...
							AV	3.05	3.20	3.85	...
IC 418	SO	...	4.10	IC 4634	AE2	4.29	...	3.25	...
	AC83	...	2.98	3.75	...		AC83	3.94	...	3.61	...
	AC79 E	4.41	...	3.85	...		AV	4.08	...	3.43	...
	AC79 N	4.41	...	3.71	...	IC 4642	AWR	...	2.58
	AE2 1	3.80	...	3.96	...	IC 4732	AK83	4.16	...	3.74	...
	AE2 2	4.12	...	IC 4776	AKI	...	3.54	...	4.24
	AW70	4.17	...		AC83	4.17	...	3.82	...
	BR F	3.77	...		AV	4.17	3.54	3.82	4.24
	AHX	3.93	IC 4846	AC79	3.64	3.78	3.93	3.93
	WD	3.63		AKI	...	3.77	...	3.70
	AV	3.94	3.33	3.89	...		AE2	3.67	...	3.98	...
IC 1747	AC79	3.51	3.23	3.26	...		BAR	3.61
	CA70	...	3.24		AV	3.64	3.77	3.95	3.82
	AW70 A	3.81	...	IC 4997	AE2	4.64	...	4.36	...
	AW70 B	2.97	...		AW70	4.23	...
	AE2 1	3.80		AHX	3.73
	AE2 2	3.40		AV	4.01	...	4.29	...
	C	3.44	IC 5117	AC79	4.64	...	4.83	4.76
	AV	3.54	3.23	3.37	3.44		AE2	3.84	...	5.07	...
IC 2003	AC79	4.01	...	3.56	3.47		AW70	4.73	...
	AC83	3.91	...	3.59	...		A	4.03
	AE2	3.79	...	3.60	...		AV	4.09	...	4.86	4.32
	AW70 SB	3.58	...	IC 5217	AC79	4.03	3.70	3.67	3.62
	AW70 WB	3.04	...		LU	...	3.75
	BAR	3.26		AE2	3.98	...	3.79	...
	A	3.42		AW70	3.62	...
	AC70	3.37		BAR	3.21
	TPP	3.06		FR1	3.41	3.46
	AV	3.67	...	3.49	3.35		A	3.66
IC 2149	BAR	3.59	3.35		CAL P	3.99
	OS	...	3.26		CAL PG	3.77
	TPP	3.67		AV	3.57	3.73	3.69	3.71
	WD	3.64	B 1	BB 2	...	3.06
	AV	3.63	3.30	B 30	AUV	...	3.62
IC 2165	KCA	...	3.26	...	3.25	CN2 1	AK83	4.00	...	3.97	...
	AC79	3.60	3.25	3.56	3.45	CN3 1	BAR	...	3.31
	AE2	3.56	...	3.66	...		SO	...	3.36
	AW70	3.73	...		AC79	3.99	...	4.01	...
	A	3.54						
	CSAS	3.76						
	MA L	3.54						
	MA MW	3.47						
	AV	3.58	3.26	3.65	3.51						
IC 3568	LACD	...	3.53	...	3.49						
	AE2	3.31	...						
	AV	...	3.53	3.31	3.49						

TABLE 2—Continued

Nebula (1)	Ref (2)	[S II] (3)	[O II] (4)	[Cl III] (5)	[Ar IV] (6)	Nebula (1)	Ref (2)	[S II] (3)	[O II] (4)	[Cl III] (5)	[Ar IV] (6)	
CN3	1 (cont.)					J	320 (cont.)					
	KON2	3.23	...	3.79	3.42		BAR	3.07	
	FR1	3.78		AC83	3.64	
	AV	3.58	3.33	3.90	3.42		AV	3.23	...	3.35	3.34	
H1	18 AK83	3.97	J	900 AC79	3.60	...	3.60	3.43	
H1	23 AK83	3.44		AE2	3.55	...	3.74	...	
H1	65 AK83	4.09		AW70	3.28	...	
H2	78 AK83	3.03		AC83	3.56	
HA1	55 PRI 2	3.48		AV	3.57	...	3.54	3.43	
HA1	59 WB2	...	3.13	K3	61 AK83	3.60	...	3.63	...	
HA4	1 MI69	...	2.67		KALS	2.96	
	HM2	2.44		AV	3.24	...	3.63	...	
	TPP2	2.84	M1	1 AC79	3.63	3.05	
	AV	2.65	2.67		AKI	...	3.08	...	2.78	
HB	6 KON	2.91	...	3.82	...		AE2	3.68	
HB	12 AC79	3.96	3.37	3.94	3.48		AV	3.66	3.07	...	2.78	
	AC83	3.74	...	3.81	...	M1	4 AK83	3.79	...	3.58	...	
	BAR	3.72		AE2	4.64	
	AV	3.80	3.37	3.88	3.48		AV	4.04	...	3.58	...	
HE1	2 KON2	3.61	M1	5 KON	3.22	...	3.42	...	
HE1	5 HM3	2.29		BAR	3.45	
HE2	131 TPP	4.38		AV	3.33	...	3.42	...	
HU1	1 AC79	3.20	...	3.36	3.01	M1	6 KON2	3.38	...	4.03	...	
	AE2	3.18	...	3.09	...		M1	8 KON	2.77	3.75
	AW70	2.49	...		M1	9 KON	3.73	...	3.99	...
	BAR	3.30	M1	11 KON2	3.21	...	
	KON	3.00		M1	12 KON2	3.87	...
	AV	3.16	...	3.08	3.01	M1	14 KON	3.70	
HU1	2 AC79	3.78	...	3.78	3.51	M1	16 KON	2.94	3.66	
	AE2	3.78	...	3.78	...		M1	17 KON	3.80
	AW70	3.59	...		M1	33 KON	4.24
	AC83	3.79		M1	35 WB2	...	3.33
	CSAS	3.42		M1	38 AK83	4.10
	AV	3.78	...	3.71	3.46		M1	41 D04 2A	3.15
HU2	1 S0	...	3.79			D04 2B	2.36
	AC79	3.41	...			AV	2.77
	AC83	3.41	...	M1	42 WB2	...	3.57	
	BAR	3.41		M1	44 AK83	3.20
	FR1	4.01							
	AV	3.89	3.79	3.41	...							
J	320 AW70	3.35	...							
	AC79	3.06	3.34							

TABLE 2—Continued

Nebula (1)	Ref (2)	[S II] (3)	[O II] (4)	[Cl III] (5)	[Ar IV] (6)	Nebula (1)	Ref (2)	[S II] (3)	[O II] (4)	[Cl III] (5)	[Ar IV] (6)
M1	65 KON2	3.62	...	3.33	...	NA	1 KON	3.71	3.77
M1	67 BAR	3.10	PS	1 OP	...	3.22
							OS	...	3.47
							AV	...	3.34
M1	71 KON	3.66	S	176 SMB 21	2.24
							SMB 22	2.12
							SMB 23	2.20
							AV	2.19
M1	74 LU	...	3.60	SN	1 BAR	2.89
	AC79	4.43	...	4.43	...		KON	3.94
	BAR	4.68		AV	2.89	3.94
	AV	4.54	3.60	4.43	...						
M1	80 KON	3.02	SS	1 AE2	4.65	...
	ORF	3.15	VV1	4 SH 2	2.53
	AV	3.08	VY1	1 KON	3.53	...
M2	6 AK83	3.67	VY1	2 BAR	3.31
							KON	3.14
M2	9 BAR NB	3.55		AV	3.22
	BAR SB	3.44	VY2	3 KON	3.47
	AV	3.50	YM	29 LZ2	2.26
M2	10 AK83	3.50	NS	5 WB2	...	3.16
M2	33 AK83	2.92	NS	67 DK 2	3.42
M2	47 KON	3.44	P	7 DK 2	2.98
M2	50 SH 2	2.81	P	33 DK 2	2.08	2.89
M3	15 AK83	3.62						
M3	20 WB2	...	3.18						
	AK83	3.73						
	AV	3.73	3.18						
M3	35 BAR	3.85						
	KON	3.92						
	AV	3.88						
M4	3 AK83	3.50						
M4	18 SAB42	3.25						
ME1	1 AKI	...	3.54	...	3.70						
	A	3.89						
	R	3.60						
	AV	...	3.54	...	3.73						
ME2	1 AC70	...	2.98						
	AKC 2	3.30	2.97	3.17	...						
	AV	3.30	2.97	3.17	...						
ME2	2 SO	...	3.71						
	AK83	3.41	...	3.77	...						
	BAR	2.83						
	AV	3.10	3.71	3.77	...						

have come from the same paper and have come from observations of the same nebular position.

We break the comparison down further in these tables by looking first at all the data regardless of the limits to the curves shown in Figure 5 (subscript 1) and then only at the nebulae in which *both* densities fall within the restricted, or acceptable, domains (subscript 2). Column (1) then gives the first ion, X , column (2) the second ion, Y , and columns (3) and (4) the number of objects available for the comparisons, N_1 and N_2 ,

respectively, for the whole domains of the theoretical curves and then for the reliable parts of the domains. In columns (5) and (6) we show the ratios for the whole and restricted ranges as in equation (1). Finally, in columns (7) and (8) we give R_1 and R_2 , the linear correlation coefficients of the logarithmic densities, again for the complete and restricted ranges. The coefficient would be 1 for perfectly correlated data, and 0 if no correlation were to exist.

The comparative study of densities is also presented graphi-

TABLE 3

COMPARATIVE ANALYSIS OF ELECTRON DENSITIES: AVERAGED DATA^a

X (1)	Y (2)	N_1^b (3)	N_2^c (4)	C_1^b (5)	C_2^c (6)	R_1^b (7)	R_2^c (8)
[O II]	[Cl III]	40	30	0.652	0.763	0.428	0.323
[O II]	[S II]	49	34	0.950	1.179	0.713	0.515
[O II]	[Ar IV]	39	14	0.818	0.753	0.366	0.350
[Cl III]	[S II]	68	32	2.498	1.333	0.483	0.357
[Cl III]	[Ar IV]	43	30	1.398	1.312	0.707	0.681
[S II]	[Ar IV]	48	18	1.133	1.129	0.443	0.053

^a The ratios, C, are the densities from ion X divided by those from ion Y.^b (1)-full data set.^c (2)-restricted data set.

cally in Figures 6 through 11, where we plot the average densities (AV from Table 2) for individual nebulae derived from one ion against those derived from another. In these figures, the filled symbols represent the restricted sample of densities that have been calculated in the range in which the theoretical curves for both ions under consideration are simultaneously reliable.

Although the points in the figures clearly correlate with one another, the scatter is very large. Most of it is probably caused by observational errors; an error of $\pm 20\%$ in the intensity ratio will produce an error of roughly ± 0.25 dex in density, or a factor of 80%, even in the most reliable parts of the curves. Compounding these errors quadratically leads to a scatter of the order of ± 0.4 dex from the mean line, which encompasses the majority of points. Additional scatter will be caused by comparison of the densities taken from different regions in inhomogeneous nebulae.

Among these plots, the ones that show the [O II] electron density as the abscissa demonstrate clearly that the [O II] values are systematically lower than the ones derived from the other ions. From Figure 6 and from Table 2, we see that only 10% of the averaged [O II] electron densities are higher than the corresponding densities from [Cl III]. The correlation coefficient is also very low. A better correlation occurs when comparing [O II] and [S II] electron densities (Fig. 7). In this case, 30% of the [O II] densities are higher than the [S II] values. If we consider only the filled triangles the percentage goes up to more than 40%, but the correlation coefficient among the logarithmic densities goes down, as the range is restricted and the number of objects reduced. Nevertheless, it is still high enough to consider the two quantities well correlated. In Figure 8, we can see that the [Ar IV] and the [O II] densities can be properly compared only for a small portion of the total sample. Even for the 14 objects for which we can perform the comparison, the correlation coefficient is only 0.35.

The [Cl III] electron densities correlate less satisfactorily with the [S II] ones than with the [Ar IV] ones (Figs. 9 and 10). In Figure 10, the nebulae are nicely distributed along the 45° line, and almost 90% of the objects lie within the half order of magnitude error bar, quite satisfactory considering the inherent observational errors. The correlation coefficients in Table 3 show that these two ions give the best agreement among our sample. Although the majority of the objects in Figure 11 seem to be correlated, the effect is deceptive. [Ar IV] and [S II] show the worst overlap. In the region of low density where [S II] is still useful, the [Ar IV] ratio is near the limit, and the densities are all generally "low" but have little actual meaning. The reverse is true at high densities. The restricted sample has no

TABLE 4

COMPARATIVE ANALYSIS OF ELECTRON DENSITIES: DATA FROM SAME REFERENCE

X (1)	Y (2)	N_1^a (3)	N_2^b (4)	C_1^a (5)	C_2^b (6)	R_1^a (7)	R_2^b (8)
[O II]	[Cl III]	25	17	0.787	0.784	0.731	0.441
[O II]	[S II]	28	24	0.840	0.916	0.731	0.509
[O II]	[Ar IV]	47	18	1.098	0.960	0.244	0.387
[Cl III]	[S II]	104	47	1.663	1.210	0.559	0.593
[Cl III]	[Ar IV]	33	24	1.436	1.317	0.786	0.702
[S II]	[Ar IV]	42	12	1.489	1.100	0.661	0.576

^a (1)-full data set.^b (2)-restricted data set.

REFERENCES.—A: Aller 1951; A41: Aller 1941; AC70: Aller and Czyzak 1970; AC79: Aller and Czyzak 1979; AC83: Aller and Czyzak 1983; ACB: Aller, Czyzak, and Buerger 1970; ACBL: Aller, Czyzak, Buerger, and Lee 1972; ACCK: Aller, Czyzak, Craine, and Kaler 1973; ACP: Allen and Czyzak 1973; ACPG: Aller and Czyzak 1973; AE: Aller and Epps 1975; AE2: Aller and Epps 1976; AF: Aller and Faulkner 1964; AH: Andrillat 1955; AHX: Andrillat and Houziaux 1968; AK1: Aller and Kaler 1964a; AK2: Aller and Kaler 1964b; AK82: Aller and Keyes 1987; AKB: Aller, Kaler, and Bowen 1966; AKC: Aller, Keyes, and Czyzak 1981; AKCS: Aller, Keyes, Czyzak, and Shields 1981; AKRC: Aller, Krupp, and Czyzak 1969; AKRM: Aller, Keyes, Ross, O'Mara 1981; AS: Aller 1969; AUV: Aller, Ufford, and Van Vleck 1949; AW: Aller and Walker 1965; AW70: Aller and Walker 1970; AWL: Aller and Wares 1969; BAR: Barker 1978; BAR4: Barker 1980; BB: Boeshaar and Bond 1977; BCA: Boeshaar, Czyzak, and Aller 1975; BR: Boeshaar 1974; C: Chopinet 1963; CA70: Czyzak and Aller 1970; CA79: Czyzak and Aller 1979; CAK1: Aller, Czyzak, and Kaler 1968; CAK2: Czyzak, Aller, and Kaler 1968; CAK4: Czyzak, Aller, and Kaler 1971; CAKF: Czyzak, Aller, Kaler, and Faulkner 1966; CAL: Czyzak, Aller, and Leckrone 1969; CEBA: Czyzak, Buerger, and Aller 1975; CSAS: Czyzak, Sonnenborn, Aller, and Sheckman 1980; DG75: Dopita and Gibbons 1975; DK: Dufour and Killen 1977; DO4: Dopita 1977; DOK: Doroshenko and Kolotilov 1973; DRS: Davies, Ring, and Selby 1964; FR1: French 1981; HAC: Heap, Aller, and Czyzak 1969; HAW2: Hawley 1978; HM: Hawley and Miller 1977; HM2: Hawley and Miller 1978a; HM3: Hawley and Miller 1978b; HM4: Hawley and Miller 1978c; KACE: Kaler, Aller, Czyzak, and Epps 1976; KCA: Kaler, Czyzak, and Aller 1968; KON: Kondratyeva 1978; KON2: Kondratyeva 1979; KALS: Kondratyeva *et al.* 1980; LA: Liller and Aller 1963; LACD: Lee, Aller, Czyzak, and Duvall 1969; LAKC: Lee, Aller, Kaler, and Czyzak 1974; LU: Lutz 1974; LU2: Lutz 1977; LZ2: Leibowitz 1975; MA: Minkowski and Aller 1956; MI69: Miller 1969; MI71: Miller 1971; MO: Minkowski and Osterbrock 1960; NOS32: Noskova 1976; O: O'Dell 1963; OA: Oliver and Aller 1969; OP: O'Dell, Peimbert, and Kinman 1964; OPC: O'Dell 1964; ORF: D'Odorico, Rubin, and Ford 1973; OS: Osterbrock 1960; PRI: Price 1981; R: Razmadze 1960; RM: Ringuet and Mendez 1973; SAB2: Sabbadin 1976; SAB4: Sabbadin 1980; SH: Sabbadin and Hamzaoglu 1981; SMB: Sabbadin, Minello, and Bianchini 1977; SO: Seaton and Osterbrock 1957; TAM: Tamura 1970; TPP: Torres-Peimbert and Peimbert 1977; TPP2: Torres-Peimbert and Peimbert 1979; WB2: Webster 1976; WD: Weedman 1968; WR: Warner and Rubin 1975; ZI2: Zipoy 1976.

correlation at all, being R less than 0.1, since the overlapping regions are so small.

Analogous plots made by using densities from the same references are shown in Figures 12 through 17. We would expect the scatter to be lower since stratification and density gradients should play a lesser role, and it is. In almost all cases the correlation coefficients in Table 4 are comparable to, or larger than, those in Table 3, in spite of the significantly lower number of points, showing clearly that some of the scatter in Figures 6 through 11 is due to features of the nebular structures, such as filaments, bars, and envelopes.

Even with the employment of the same-reference data for oxygen and chlorine (Fig. 12), which are once again a small part of the total sample, the [O II] values average less than those from [Cl III]. From Figure 13 we see that the densities from [O II] and [S II] compare better than they did for the

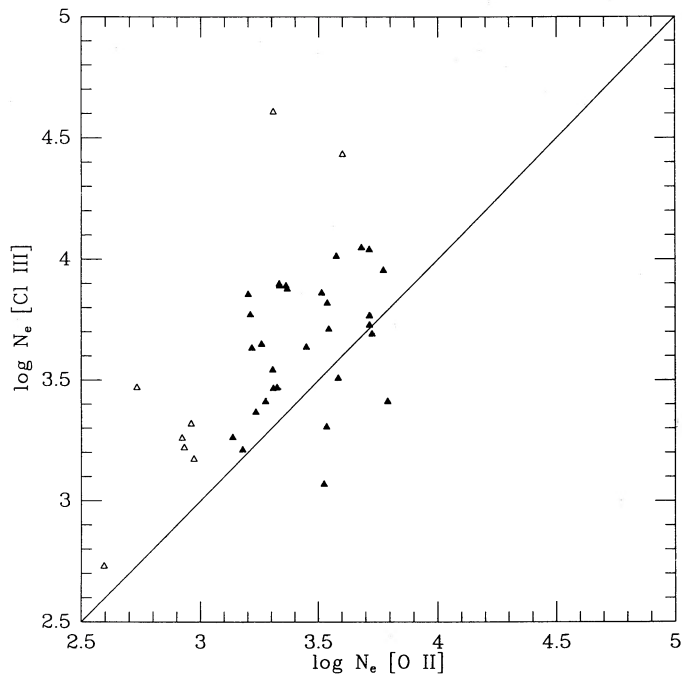


FIG. 6

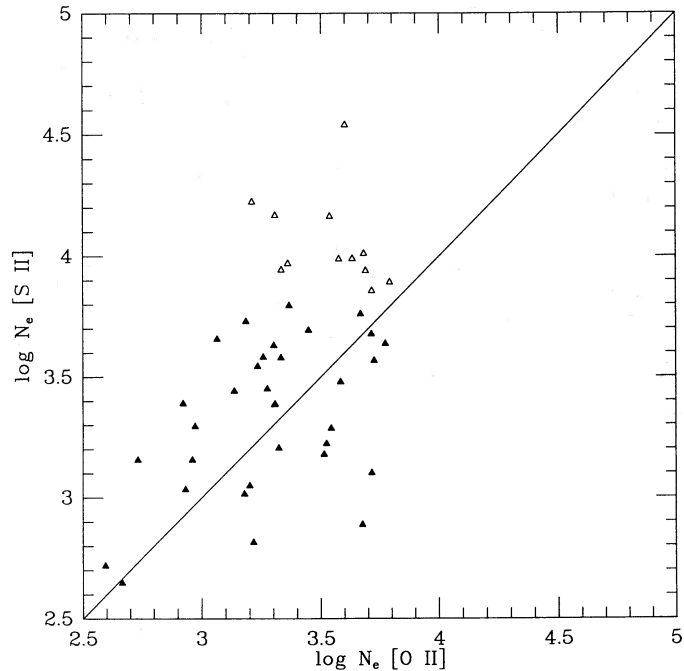


FIG. 7

FIG. 6.— N_e [Cl III] vs. N_e [O II] for the averages in (AV) Table 2. The filled symbols represent the densities derived from intensity ratios that are within the reliability limits for both ions.

FIG. 7.— N_e [S II] vs. N_e [O II] for the averages (AV) in Table 2. See the caption to Fig. 6.

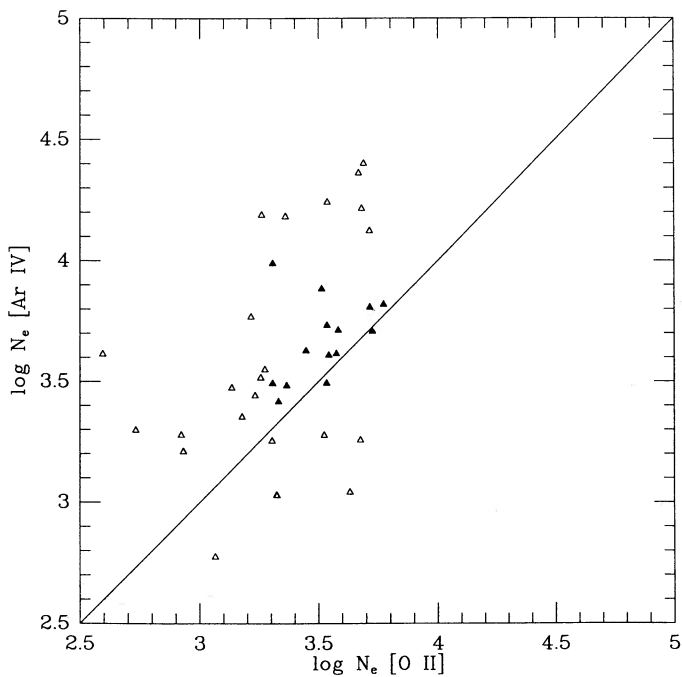


FIG. 8

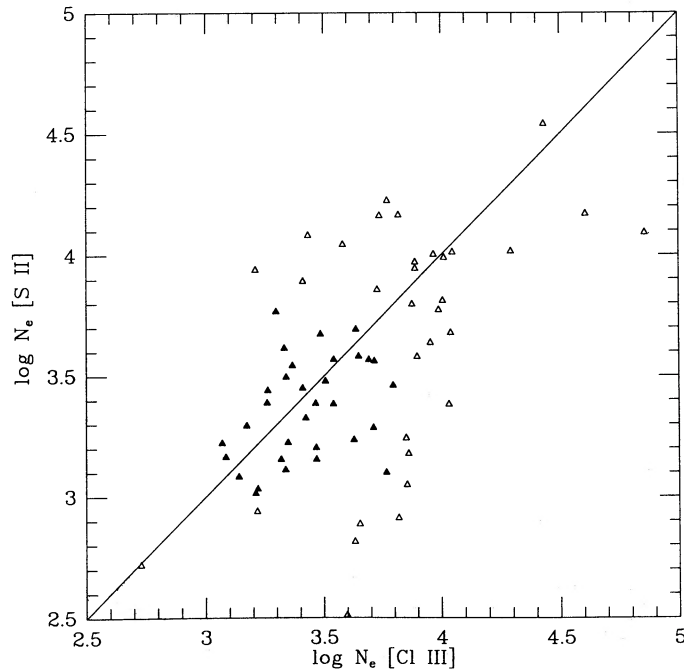


FIG. 9

FIG. 8.— N_e [Ar IV] vs. N_e [O II] for the averages (AV) in Table 2. See the caption to Fig. 6.

FIG. 9.— N_e [S II] vs. N_e [Cl III] for the averages (AV) in Table 2. See the caption to Fig. 6.

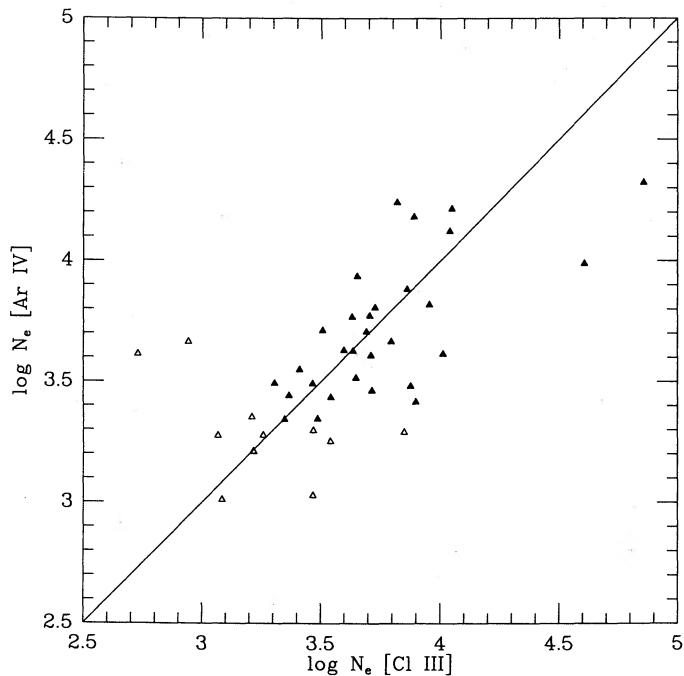


FIG. 10

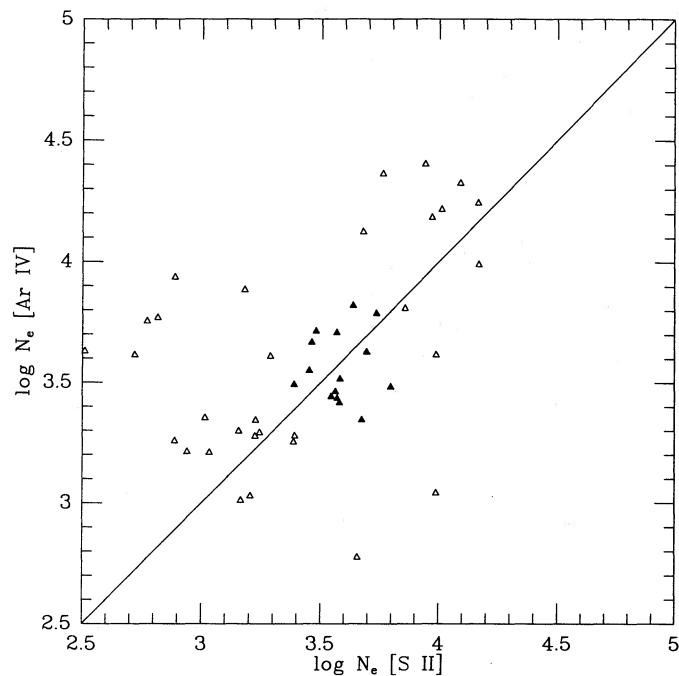


FIG. 11

FIG. 10.— N_e [Ar IV] vs. [Cl III] for the averages (AV) in Table 2. See the caption to Fig. 6.

FIG. 11.— N_e [Ar IV] vs. N_e [S II] for the averages (AV) in Table 2. See the caption to Fig. 6.

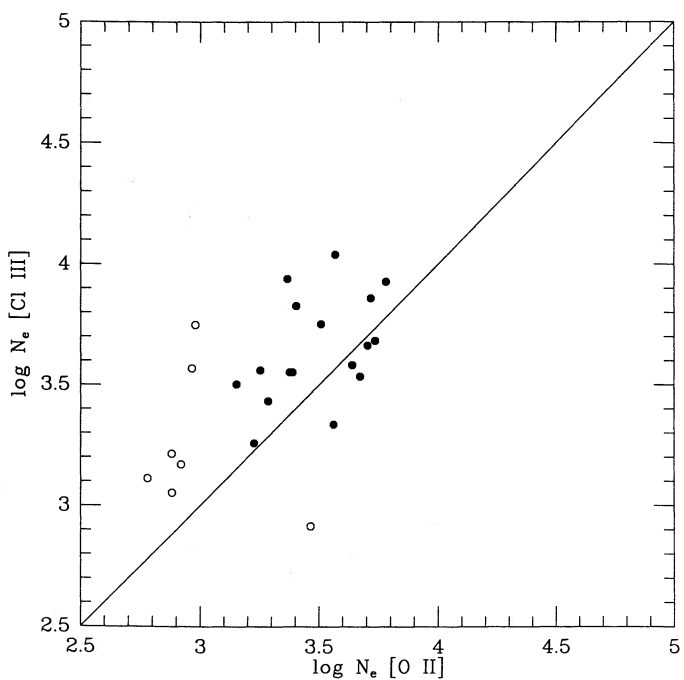


FIG. 12

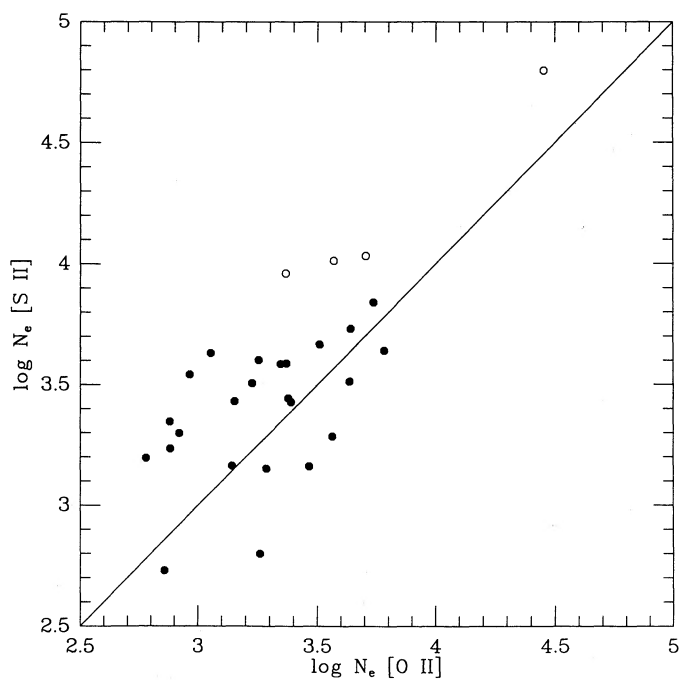


FIG. 13

FIG. 12.— N_e [Cl III] vs. N_e [O II] for all electron densities for which each ion was observed in common. The filled symbols represent the densities derived from intensity ratios that are within the reliability limits for each ion.

FIG. 13.— N_e [S II] vs. N_e [O II] for all electron densities for which each ion was observed in common. See the caption to Fig. 12.

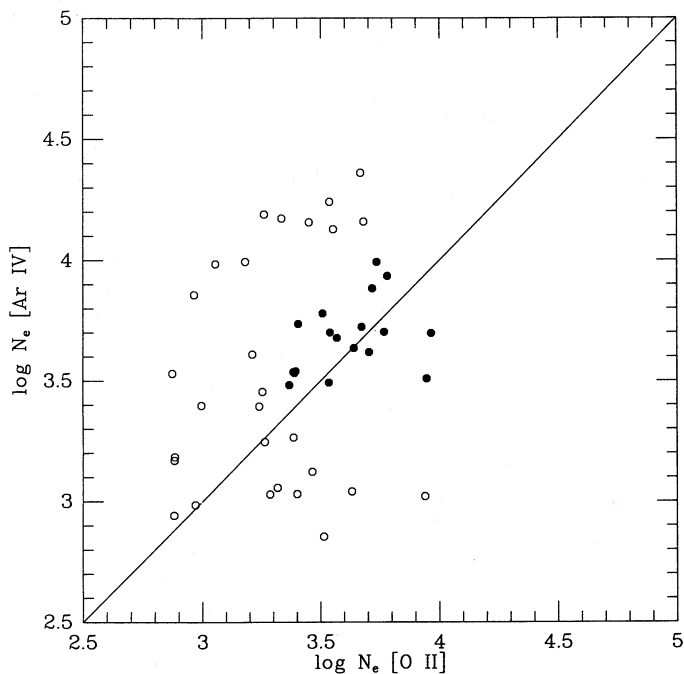


FIG. 14

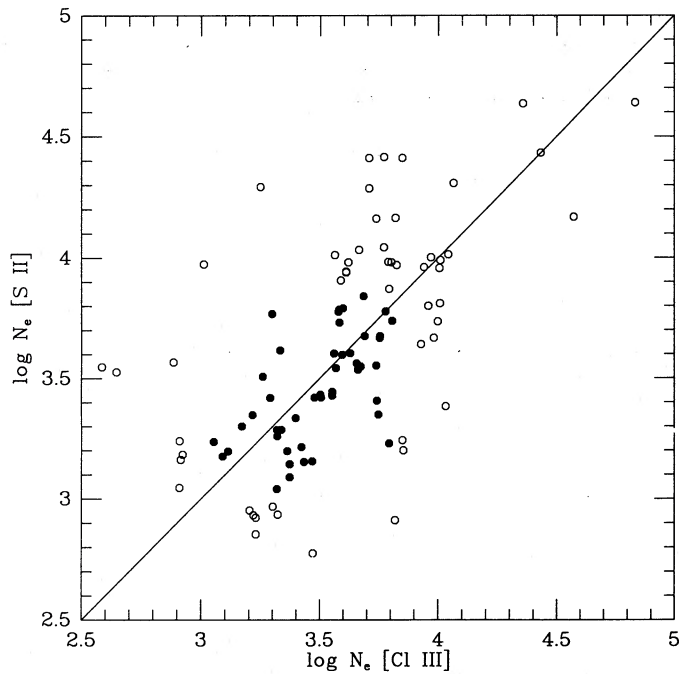


FIG. 15

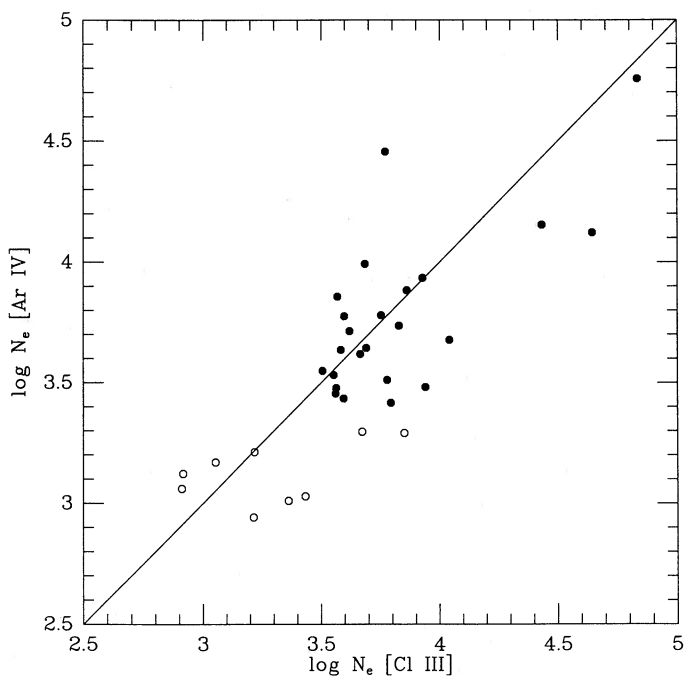
FIG. 14.— $N_e [\text{Ar IV}]$ vs. $N_e [\text{O II}]$ for all electron densities for which each ion was observed in common. See the caption to Fig. 12.FIG. 15.— $N_e [\text{S II}]$ vs. $N_e [\text{Cl III}]$ for all electron densities for which each ion was observed in common. See the caption to Fig. 12.

FIG. 16

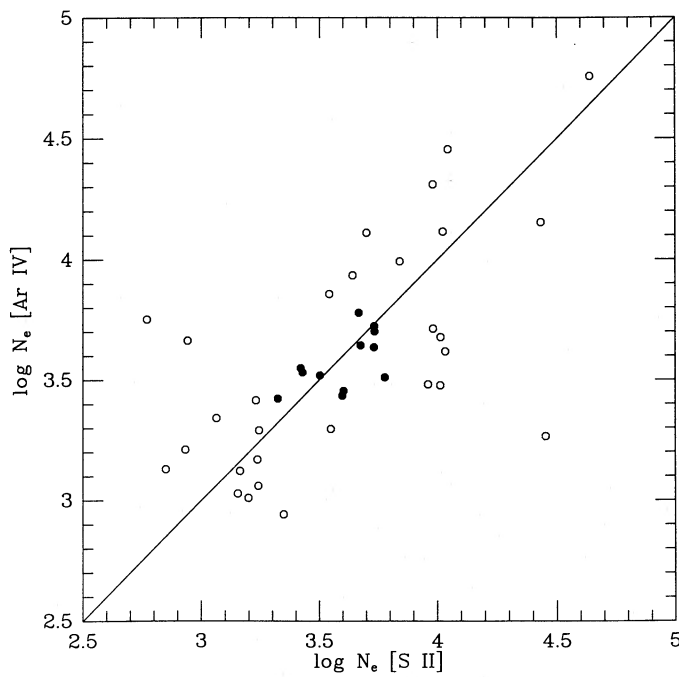


FIG. 17

FIG. 16.— $N_e [\text{Ar IV}]$ vs. $N_e [\text{Cl III}]$ for all electron densities for which each ion was observed in common. See the caption to Fig. 12.FIG. 17.— $N_e [\text{Ar IV}]$ vs. $N_e [\text{S II}]$ for all electron densities for which each ion was observed in common. See the caption to Fig. 12.

averaged data, but the oxygen densities are still somewhat low. Figure 14 shows that electron densities from [O II] and [Ar IV] are not well correlated because the density regimes do not sufficiently overlap (see Table 4).

In Figure 15, we relate electron densities from [Cl III] and [S II] as measured in the same positions in the nebulae. The correlation, both for the full and restricted sets, is only fair. The [S II] and [Ar IV] comparison is little better in Figure 17, still because of the very restricted overlap, but it is much better than in the analogous plot in Figure 11: compare Tables 3 and 4. Finally, the argon electron densities appear to be well correlated with those from [Cl III] (Fig. 16) when all data for a given object are taken from the same positions. The index of correlation for both the full and restricted samples is again the best of all, with a coefficient of 0.7.

IV. DISCUSSION

Assuming that no gradients exist, that is that all nebulae are homogeneous, we see from Table 4 (the better source) that at worst all the ions give densities that are within about 30% of one another. We conclude that the current parameters actually give quite good results, especially in view of the potential for observational errors. In particular, the [Ar IV] doublet ratios, calculated with the collision strengths of Zeippen, Butler, and LeBourlot (1987) now appear to give useful results. The differences in the densities derived from the different ions could still be produced by residual, small errors in the atomic parameters.

In order to examine the density comparisons (and the possibility of errors in the atomic parameters) more fully, the data must be compared with existing ionization and hydrodynamic models of PNe. On the assumption that the nebulae start out as uniform shells or rings, whose densities decrease from inside out according to $1/r^2$, the different forbidden line ratios would give different electron densities as a function of the distance from the central star to the region in which the lines originate. In this approximation, the ion with the highest potential of ionization Ar^{+3} (40.7 eV) would characterize the innermost zones of the nebulae, and Cl^{+2} (23.8 eV), O^+ (13.6 eV), and S^+ (10.4 eV) would be progressively in the outer parts, the last marking zones in the neighborhoods of the hydrogen ionization fronts.

By studying Tables 3 and 4 we infer that, among the better correlated electron densities, the differences in density are not in the direction expected from a simple analysis on the basis of the ionization potentials. The sequence $N_e[\text{Ar IV}] > N_e[\text{Cl III}] > N_e[\text{O II}] > N_e[\text{S II}]$ is not reproduced in most of the sample. From both Tables 3 and 4 we see that [Cl III] consistently gives the highest densities. In Table 4, $N_e[\text{Ar IV}]$ is actually lower than any of the others, the sequence going $N_e[\text{Cl III}] > N_e[\text{S II}] > N_e[\text{O II}] > N_e[\text{Ar IV}]$. Note, however, that the comparisons are not internally consistent, since different nebulae are used to construct different ratios. In Table 3, for example, $N_e[\text{Cl III}]$ is larger than $N_e[\text{Ar IV}]$ and $N_e[\text{O II}]$ by the same amount for the objects so studied, but for another (overlapping) set, $N_e[\text{Ar IV}]$ is substantially greater than $N_e[\text{O II}]$.

One of the results, that $N_e[\text{S II}] > N_e[\text{O II}]$, may have a ready explanation. Rubin (1989) shows that the inequality $N_e[\text{S II}] < N_e[\text{O II}]$ is independent of the density distribution of the nebula as long as there is no stratification. If the front is subsonic with respect to the nebular motion, it is of the D-type, with higher densities beyond the front itself. The [O II] for-

bidden lines, which are produced from just inside the inner boundary of the planetary nebula to the hydrogen ionization front, would then mark, on the average, a more rarefied zone than the [S II] lines, which are produced at or just beyond the hydrogen ionization front, in the outer parts of the nebula.

If this scenario is correct, we might expect to see a difference in the $N_e[\text{O II}]/N_e[\text{S II}]$ ratio between optically thick nebulae, those that have demonstrable ionization fronts, and those that are optically thin. The thick nebulae are characterized by strong [O II] and [S II], and consistently, by a small Zanstra discrepancy (the ratio of the He II and H Zanstra temperatures), that is, the two Zanstra temperatures should be similar (see Kaler 1983). Plots of the above density ratio against both the strength of [O II] $\lambda 3727$ and the Zanstra discrepancy show no significant correlation, which might lend some credence to the suggestion that the atomic parameters still contain small errors.

Chlorine densities are consistently higher than the argon ones, for both the selected and unselected data sets. The low [Ar IV] electron densities might be due to a dynamic effect. Giuliani (1981) evolves hydrodynamic models of planetary nebulae in which colliding winds and ionization fronts are considered. The results show that, in all cases, the ionization front produces a rarefaction at the inner boundary of the nebula. The results mentioned above are consistent with Ar^{+3} being formed in a central hole that is typical of many nebular structures. Whenever the [Ar IV] lines are observed, then, they may be produced in the inner part of the plasma, so that the relative lower electron density should be expected if the hydrodynamic model reflects the situation observed. We do not know the appropriate electron temperature to use for [Ar IV]. However, electron temperature gradients should not be a factor since the densities are not very dependent on T_e . Of course any of these speculations are compromised by possible errors in the atomic data. Nevertheless, the density ratios at least have physical explanations of some sort, which makes the atomic calculations look quite satisfactory.

Finally, Rubin (1986) suggested that the [O II] doublet might be affected by electrons that enter the metastable states by recombination. Since the recombination rates depend inversely on the electron temperature, the densities derived from the lines would be erroneous at low temperatures and converge to the correct values at high. The ratio of $N_e[\text{O II}]/N_e[\text{S II}]$ shows no dependency on T_e as derived from [O III], but this is a weak test as the [O III] temperature is not appropriate to the N^+ and O^+ regions, and $T_e[\text{N II}]$ and $T_e[\text{O III}]$ do not behave in the same way (Kaler 1986). The number of nebulae for which $T_e[\text{N II}]$ is known is insufficient to provide a significant test. The general agreement among all densities suggests that recombination is not an important factor, but more data are clearly needed.

In summary, we can infer the following conclusions and open questions from our study of electron densities of a large sample of planetary nebulae. The [O II] densities are reliable for a large range of values, and they are very close to the [S II] ones, though the latter seem to be slightly higher than what we would expect from a steady decrease in density with increasing radius. The effect of recombination on the [O II] lines cannot be ruled out, but the process does not seem at least to be a large factor. The higher [S II] densities may arise from a snow-plow effect at the ionization front. The [S II] densities are reliable in a fairly small range ($2.45 < \log N_e < 3.85$), and in the overlap range they correlate reasonably well with the

[Cl III] ones, when both densities are from the same data set. [Ar IV] and [Cl III] electron densities correlate well, and have reasonably similar values, and their theoretical curves have similar domains for a large range of values. The systematically slightly lower [Ar IV] densities might be due to a hydrodynamic effect. Generally the atomic data seem to be satisfactory, though small errors are still allowed by the observations.

The next step in this continuing quest for measured densities is greater precision in the observations, so as to reduce the scatter and provide a finer check on the comparisons of the

densities derived from one ion with those derived from another.

This work was supported by National Science Foundation grants AST 84-19355 and AST 88-13686 to the University of Illinois. We would like to thank C. J. Zeippen and R. Rubin for encouragement and for communicating results in advance of publication and again R. Rubin for valuable commentary on the manuscript. We would also like to thank D. Pommert and N. Killeen for help in constructing Table 2.

REFERENCES

- Aller, L. H. 1941, *Ap. J.*, **93**, 236.
 ———. 1951, *Ap. J.*, **113**, 125.
 ———. 1969, *Sky Tel.*, **37**, 348.
 Aller, L. H., and Czyzak, S. J. 1970, *Ap. J.*, **160**, 929.
 ———. 1973, private communication.
 ———. 1979, *Ap. Space Sci.*, **62**, 397.
 ———. 1983, *Ap. J. Suppl.*, **51**, 211.
 Aller, L. H., Czyzak, S. J., and Buerger, E. C. 1970, *Ap. J.*, **162**, 783.
 Aller, L. H., Czyzak, S. J., Buerger, E. G., and Lee, P. 1972, *Ap. J.*, **172**, 361.
 Aller, L. H., Czyzak, S. J., Craine, E., and Kaler, J. B. 1973, *Ap. J.*, **182**, 509.
 Aller, L. H., Czyzak, S. J., and Kaler, J. B. 1968, *Ap. J.*, **151**, 187.
 Aller, L. H., and Epps, H. W. 1975, *Ap. J.*, **197**, 175.
 ———. 1976, *Ap. J.*, **204**, 445.
 Aller, L. H., and Faulkner, D. J. 1968, *IAU-URST Symposium 20, The Galaxy and the Magellanic Clouds*, ed. F. J. Kerr and A. W. Rodgers (Camberra: Aust. Acad. of Sci.).
 Aller, L. H., and Kaler, J. B. 1964a, *Ap. J.*, **139**, 1074.
 ———. 1964b, *Ap. J.*, **140**, 621.
 Aller, L. H., Kaler, J. B., and Bowen, I. S. 1966, *Ap. J.*, **144**, 291.
 Aller, L. H., and Keyes, C. D. 1987, *Ap. J. Suppl.*, **65**, 405.
 Aller, L. H., Keyes, C. D., and Czyzak, S. J. 1981, *Ap. J.*, **250**, 596.
 Aller, L. H., Keyes, C. D., Czyzak, S. J., and Shields, J. A. 1981, *Ap. J.*, **248**, 569.
 Aller, L. H., Keyes, C., Ross, J., and O'Mara, B. 1981, *M.N.R.A.S.*, **197**, 647.
 Aller, L. H., Krupp, E., and Czyzak, S. J. 1969, *Ap. J.*, **158**, 953.
 Aller, L. H., Ufford, C. W., and Van Vleck, J. H. 1949, *Ap. J.*, **109**, 42.
 Aller, L. H., and Walker, M. F. 1965, *Ap. J.*, **141**, 1318.
 ———. 1970, *Ap. J.*, **161**, 917.
 Aller, L. H., and Wares, G. 1969, *Nature*, **221**, 646.
 Andriillat, H. 1955, *Compte Rendus*, **243**, 702.
 Andriillat, Y., and Houziaux, L. 1968, *IAU Symp. No. 34*, 68.
 Barker, T. 1978, *Ap. J.*, **220**, 193.
 ———. 1980, *Ap. J.*, **240**, 99.
 Boeshaar, G. O. 1974, *Ap. J.*, **187**, 283.
 Boeshaar, G. O., and Bond, H. E. 1977, *Ap. J.*, **213**, 421.
 Boeshaar, G. O., Czyzak, S. J., and Aller, L. H. 1975, *Ap. J. Suppl.*, **28**, 335.
 Brocklehurst, M. 1971, *M.N.R.A.S.*, **153**, 471.
 Butler, K., and Zeippen, C. J. 1989, *Astr. Ap.*, **208**, 337.
 Chopinet, M. 1963, *J. D. Obs.*, **46**, 27.
 Czyzak, S. J., and Aller, L. H. 1970, *Ap. J.*, **162**, 495.
 Czyzak, S. J., and Aller, L. H. 1979, *M.N.R.A.S.*, **188**, 229.
 Czyzak, S. J., Aller, L. H., and Kaler, J. B. 1968, *Ap. J.*, **154**, 543.
 ———. 1971, *Ap. J.*, **168**, 405.
 Czyzak, S. J., Aller, L. H., Kaler, J. B., and Faulkner, D. J. 1966, *Ap. J.*, **143**, 327.
 Czyzak, S. J., Aller, L. H., and Leckrone, D. 1969, *Ap. J.*, **157**, 1225.
 Czyzak, S. J., Buerger, E. G., and Aller, L. H. 1975, *Ap. J.*, **198**, 431.
 Czyzak, S. J., Sonnenborn, G., Aller, L. H., and Schectman, S. A. 1980, *Ap. J.*, **241**, 719.
 Davies, L. B., Ring, J., and Selby, M. J. 1964, *M.N.R.A.S.*, **50**, 1186.
 Dopita, M. A. 1977, *Ap. Space Sci.*, **48**, 437.
 Dopita, M. A., and Gibbons, A. H. 1975, *M.N.R.A.S.*, **171**, 73.
 D'Odorico, S., Rubin, V. C., and Ford, W. C. 1973, *Astr. Ap.*, **22**, 469.
 Doroshenko, V. T., and Kolotilov, E. A. 1973, *Astr. Zh.*, **50**, 1186.
 Dufour, R. J., and Killen, R. M. 1977, *Ap. J.*, **211**, 68.
 French, H. B. 1981, *Ap. J.*, **246**, 434.
 Giuliani, J. L., Jr. 1981, *Ap. J.*, **245**, 903.
 Hawley, S. A. 1978, *Pub. A.S.P.*, **90**, 370.
 Hawley, S. A., and Miller, J. S. 1977, *Ap. J.*, **212**, 94.
 ———. 1978a, *Ap. J.*, **220**, 609.
 ———. 1978b, *Ap. J.*, **221**, 851.
 ———. 1978c, *Pub. A.S.P.*, **90**, 39.
 Heap, S., Aller, L. H., and Czyzak, S. J. 1969, *Ap. J.*, **157**, 607.
 Kaler, J. B. 1983, *Ap. J.*, **271**, 188.
 ———. 1986, *Ap. J.*, **308**, 322.
 Kaler, J. B., Aller, L. H., Czyzak, S. J., and Epps, H. W. 1976, *Ap. J. Suppl.*, **31**, 163.
 Kaler, J. B., Czyzak, S. J., and Aller, L. H. 1968, *Ap. J.*, **153**, 43.
 Kondratyeva, L. N. 1978, *Astr. Zh.*, **55**, 334.
 ———. 1979, *Astr. Zh.*, **56**, 345.
 Kondratyeva, L. N., Afanasjev, V. I., Lipovetskij, V. A., and Shapovalova, A. I. 1970, private communication.
 Krueger, T. K., and Czyzak, S. J. 1970, *Proc. Roy. Soc. London A*, **318**, 531.
 Lee, P. D., Aller, L. H., Czyzak, S. J., and Duvall, R. N. 1969, *Ap. J.*, **155**, 853.
 Lee, P. D., Aller, L. H., Kaler, J. B., and Czyzak, S. J. 1974, *Ap. J.*, **192**, 159.
 Leibowitz, E. M. 1975, *Ap. J.*, **196**, 191.
 Liller, W., and Aller, L. H. 1963, *Proc. Nat. Acad. Sci.*, **49**, 675.
 Lutz, J. H. 1974, *Pub. A.S.P.*, **86**, 888.
 ———. 1977, *Pub. A.S.P.*, **89**, 10.
 Mendoza, C. 1983, in *IAU Symposium 103, Planetary Nebulae*, ed. D. Flower (Dordrecht: Reidel), p. 245.
 Mendoza, C., and Zeippen, C. J. 1982, *M.N.R.A.S.*, **198**, 127.
 Miller, J. S. 1969, *Ap. J.*, **157**, 1215.
 ———. 1971, *Ap. J. (Letters)*, **165**, L101.
 Minkowski, R., and Aller, L. H. 1956, *Ap. J.*, **124**, 93.
 Minkowski, R., and Osterbrock, D. E. 1960, *Ap. J.*, **131**, 537.
 Noskova, R. I. 1976, *Astr. Zh.*, **53**, 1210.
 O'Dell, C. R. 1963, *Ap. J.*, **138**, 1018.
 ———. 1964, private communication.
 O'Dell, C. R., Peimbert, M., and Kinman, T. D. 1964, *Ap. J.*, **140**, 119.
 Oliver, J. P., and Aller, L. H. 1969, *Ap. J.*, **157**, 601.
 Osterbrock, D. E. 1960, *Ap. J.*, **131**, 541.
 Pradhan, A. K. 1976, *M.N.R.A.S.*, **177**, 31.
 Price, C. M. 1981, *Ap. J.*, **247**, 540.
 Razmadze, N. A. 1960, *Astr. Zh.*, **37**, 1005.
 Riguelet, A. E., and Mendez, R. H. 1973, *Pub. A.S.P.*, **85**, 96.
 Rubin, R. H. 1986, *Ap. J.*, **309**, 334.
 ———. 1989, *Ap. J. Suppl.*, **69**, 897.
 Sabbadin, F. 1976, *Astr. Ap.*, **52**, 291.
 ———. 1980, *Astr. Ap.*, **84**, 216.
 Sabbadin, F., and Hamzaoglu, E. 1981, *Astr. Ap.*, **94**, 25.
 Sabbadin, F., Minello, S., and Bianchini, A. 1977, *Astr. Ap.*, **60**, 147.
 Saraph, M., and Seaton, M. J. 1970, *M.N.R.A.S.*, **148**, 367.
 Seaton, M. J., and Osterbrock, D. E. 1957, *Ap. J.*, **125**, 66.
 Tamura, S. 1970, *Sci. Rpts., Tohoku Univ.*, Ser. 1, **53**, 10.
 Torres-Peimbert, S., and Peimbert, M. 1977, *Rev. Mex. Astr. Ap.*, **2**, 181.
 ———. 1979, *Rev. Mex. Astr. Ap.*, **4**, 341.
 Warner, J. W., and Rubin, V. C. 1968, *Ap. J.*, **198**, 593.
 Webster, B. L. 1976, *M.N.R.A.S.*, **174**, 513.
 Weedman, D. W. 1968, *Pub. A.S.P.*, **80**, 314.
 Zeippen, C. J. 1982, *M.N.R.A.S.*, **198**, 111.
 ———. 1987, *Astr. Ap.*, **173**, 410.
 Zeippen, C. J., Butler, K., and LeBourlot, J. 1987, *Astr. Ap.*, **188**, 251.
 Zipoy, D. M. 1976, *Ap. J.*, **209**, 108.

JAMES B. KALER: Department of Astronomy, 349 Astronomy Bldg., 1011 W. Springfield Ave., Urbana, IL 61801

LETIZIA STANGHELLINI: Osservatorio Astronomico di Bologna, via Zamboni 33, 40100 Bologna, Italy